

PREPARATION OF Bi₂MoO₆/KELP BIOCHAR NANOCOMPOSITE FOR ENHANCING DEGRADABILITY OF METHYLENE BLUE

ZHOU, Y.¹ – CAI, L.² – GUO, J.³ – WANG, Y.⁴ – JI, L.^{4*} – SONG, W.^{5*}

¹College of Port and Transportation Engineering, Zhejiang Ocean University
Haida South Road No.1, Lincheng Street, Dinghai District, 316022 Zhoushan, China

²College of Environmental and Science Technology, Donghua University
201620 Shanghai, China

³College of Food and Medical, Zhejiang Ocean University, 316022 Zhoushan, China

⁴Institute of Innovation & Application, Zhejiang Ocean University, 316022 Zhoushan, China

⁵College of Petrochemical and Energy Engineering, Zhejiang Ocean University
316022 Zhoushan, China

*Corresponding authors

L. Ji – e-mail: jll-gb@163.com; W. Song – e-mail: swd60@163.com
phone: +86-580-226-2589; fax: +86-580-226-2063

(Received 25th May 2018; accepted 1st Aug 2018)

Abstract. Bi₂MoO₆/kelp biochar (BKB) nanocomposite has been obtained by a combination of pyrolysis and solvothermal method. The synthesized sample was characterized by X-ray diffraction (XRD), scanning electron microscopy (SEM), UV-vis diffuse reflection spectroscopy (DRS) and Fourier transform infrared (FT-IR) spectra. The specific surface area and pore volumes of BKB nanocomposite with the mass ratio of Bi₂MoO₆ to kelp biochar of 0.25 (BKB-0.25) were 210.918 m²/g and 0.2449 cm³/g, respectively, indicating that the as-prepared nanocomposite had wide specific surface area and porous structure. Moreover, the photocatalytic tests exhibited that the highest photocatalytic degradation efficiency obtained by BKB-0.25 under visible light irradiation for 60 min was 61.39%, which was up to 13 times higher in comparison with pure Bi₂MoO₆. This showed that the photocatalytic degradation data fitted well with pseudo-first-order model. The unique features of BKB nanocomposite suggested that it may have a great potential for dyes removal from liquid effluents.

Keywords: *kelp biochar, photocatalyst, adsorption activity, nanocomposite, removal efficiency*

Introduction

Methylene blue (MB), a cationic type model dye compound, is widely used in industries such as paper, leather, cosmetics and pharmaceutical industries (Wang et al., 2018; Velanganni et al., 2018). Residues of dye without proper treatment will do harm to both human health and ecological safety (Abdelwahab and Emh, 2018; Liu et al., 2017; Ghosh and Bandyopadhyay, 2017; Fan et al., 2016). The most common methods have been used for wastewater treatment such as chemical oxidation, microbiological degradation, electrochemical treatment, adsorption, etc, but they are limited to some kinds of dyes due to many reasons. Being effective and attractive, the photocatalytic technique is a promising way for the treatment of dyes and organic compounds from aqueous effluents.

Nanostructured photocatalysts have gained worldwide attention currently, due to their potential application in environmental purification and solar energy conversion

(Zhang et al., 2006; Zhang et al., 2007; Umapathy et al., 2015). Recently, Bi₂MoO₆ has been one of the excellent photocatalysts for the degradation of organic compounds under visible light irradiation, which has excellent intrinsic properties, such as, dielectric nature, catalytic behavior and luminescence with a typical E_g of about 2.6 eV (Zhang et al., 2011). However, the photocatalytic performance of Bi₂MoO₆ is still far from satisfactory due to the high recombination rate of photogenerated electron–hole pairs and potentially poor surface chemistry, which limits the application of Bi₂MoO₆ catalysts (Yan et al., 2015). It has been demonstrated that complex or hierarchical hetero-nano-structures with high performance can be achieved to facilitate the separation of photo-generated electron–hole pairs and further improve the photocatalytic activity (Shang et al., 2010; Li et al., 2016; Chen et al., 2015; Cao et al., 2011). Among them, Bi₂MoO₆-based composites, such as MoS₂/Bi₂MoO₆, BiOI/Bi₂MoO₆ and Bi₂MoO₆/TiO₂ have been proved to have higher photocatalytic activity.

Biochar materials obtained from waste biomass (gasification or pyrolysis) show better performance in adsorption of organic pollutants from water owing to their low cost, economically feasible, developed porosity, wide specific surface area and abundant functional groups (Enniya et al., 2018; Jian et al., 2018; Yang et al., 2017). Macroalgae has been promising biomass resources for the production of activated carbon with a high adsorption capacity (Rathinam et al., 2011; Yu et al., 2015; Son et al., 2018; Lee et al., 2018; Ross et al., 2018). However, the present transformation and utilization of seaweed are mainly in the production of fertilizers, industrial gums (phytocolloids), and bio-materials for medical applications, which limits the utilization of this raw material for the production of adsorption and carrier material (Haykiri-Acma et al., 2013; Yu et al., 2017; Joonhyuk et al., 2014).

In this work, a novel Bi₂MoO₆/kelp biochar nanocomposite by using the abundant and available kelp was fabricated by a combination of pyrolysis and solvothermal method, which exhibited an enhanced photocatalytic activity in the visible light irradiation. Therefore, the as-prepared sample may be expected to effectively degrade organic pollutants in water, which could realize the value-added use of kelp biomass.

Materials and methods

Materials

The fresh kelp was collected from a local food market in Zhoushan, Zhejiang. Bi (NO₃)•5H₂O, Na₂MoO₄•H₂O, Methylene blue (MB, C₁₆H₁₈N₃SCI), glycol, ethanol (>99.7%) and hydrochloric acid were analytical grade and had been obtained from Sinopharm Chemical Reagent Co., Ltd. China.

Preparation of carbon

45 g of dried kelp powder was pyrolyzed in a tubular furnace under nitrogen flow (100 mL min⁻¹) up to 800 °C with a rate of 10 °C/min, and the final temperature lasted for 3 h (Wang et al., 2016; Aravindhana et al., 2007; Aravindhana et al., 2004; Rathinam et al., 2011). The carbonized residue was allowed to cool down to room temperature in a furnace under the same gas flow. Then, it was removed from the furnace and stored in an air-tight sample vessel (Choi et al., 2014; Yu et al., 2017; Afonso et al., 2018).

The obtained black solid was mixed with KOH powder with the mass ratio of 1:3. Then the mixture was also pyrolyzed in that tubular furnace under nitrogen flow (100 mL min⁻¹) up to 800 °C with a rate of 10 °C/min. The residence time of the final temperature would reduce to 2 h. This cooled sample was immersed in the deionization water and then heated in a water bath at 80 °C. The sample was washed with 0.1 mol/L HCl to neutrality, then filtered and washed with deionization water three times, and finally dried at 73 °C overnight.

Preparation of Bi₂MoO₆-kelp biochar nanocomposite

In a typical case, 0.363 g Bi(NO₃)₃•5H₂O and 0.0907 g Na₂MoO₄•2H₂O were dissolved in 7 mL ethylene glycol. Then, 0.1016 g kelp biochar was dispersed into 20 mL ethanol under magnetic stirring for 60 min to form a homogeneous solution, which was slowly added into the Bi(NO₃)₃•5H₂O and Na₂MoO₄•2H₂O mixed solution, stirring for 12 h. The resulting mixture was transferred into a 50 mL Teflon-lined stainless steel autoclave, heated to 160 °C and maintained for 24 h. Then, the autoclave was cooled down to room temperature. The obtained sample was washed with deionized water and ethanol to remove any ionic residual, then dried at 73 °C for 12 h. The as-fabricated sample was denoted as BKB-2.25. According to this method, the Bi₂MoO₆/kelp biochar composite with different mass ratios of 0.25, 0.75, 1.25 and 1.75 were synthesized and named as BKB-0.25, BKB-0.75, BKB-1.25 and BKB-1.75, respectively. For comparison, pure Bi₂MoO₆ was prepared by adopting the method in the absence of kelp biochar.

Characterization

Composition and morphology of the samples were investigated by scanning electron microscopy (SEM, Hitachi S-4800, Japan), and X-ray diffraction (Ultima IV X-Ray Diffractometer, Rigaku Corporation, Japan) in the range of 2θ = 10–80°. The surface functional group were analyzed by Fourier transform infrared spectra (FTIR, Nicolet 5700, Thermo Corp., USA). UV–vis spectrophotometer (UV-4100, Shimadzu) was used to analyze the optical properties of the as-fabricated materials in the wavelength range of 200–1000 nm by the diffuse-reflectance spectroscopy (DRS). The specific surface areas of the samples were measured with a Micromeritics ASAP 2010 instrument and analyzed by the BET method.

The removal efficiency of MB

The adsorption experiments of MB were investigated by adding 0.01 g as-fabricated samples to 50 mL MB solutions (80 mg/L) in Erlenmeyer flasks which were stirred in the dark for 4 h to ensure the dye and sample to reach adsorption-desorption equilibrium.

The photocatalytic activity of BKB composite was evaluated by photodegradation of MB solution under visible light (λ > 420 nm) irradiation. To obtain the needed irradiation photo source (14 V, 16 A, 15 cm), a 300 W xenon lamp (FSX-300, NBeT Group Corp. Beijing) was used as a visible light source. Moreover, 2 mL of suspension was collected followed via centrifuging to move the remained photocatalysts at specific illumination intervals. And the obtained clear solution was measured at 665 nm via a UV–vis spectroscopy (UV 2600, Shimadzu). The adsorption

capacity of BKB composite was calculated according to *Equation 1* as follows (Chen et al., 2016):

$$\text{Adsorption capacity (mg/g)} = (C_0 - C_e) \times (V/m) \quad (\text{Eq.1})$$

where q_e is equilibrium adsorption capacity of the BKB composite, mg/g; C_e and C_0 are the equilibrium and initial concentration of MB concentration, mg/L; V is the volume of the solution, L; M is the mass of the BKB composite, g.

The photocatalytic degradation of BKB composite was calculated according to *Equation 2* as follows (Geng et al., 2017):

$$\text{Degradation} = [(A_0 - A_1) / A_0] \times 100\% \quad (\text{Eq.2})$$

where A_0 is an initial photocatalytic degradation of methylene blue, A_1 is an absorbance measured at the irradiation time.

Results and discussion

Characterization of as-prepared samples

The specific surface area and pore volumes of BKB composite are listed in *Table 1*. It can be seen that the specific surface area and pore volumes increase with the decrease of Bi₂MoO₆ content. Particularly, the maximum values BKB-0.25 obtained are 210.918 m²/g and 0.2449 cm³/g, respectively, which may be beneficial for the enhancement of sorption capacity. The nitrogen adsorption isotherms for BKB-0.25 suggests the V isotherms with a hysteresis loop at $P/P_0 > 0.4$. Moreover, the slit between adsorption and desorption curves may be due to the presence of stacking holes. The pore size distribution of BKB-0.25 also exhibits the significance of mesopores with pores mainly in the range 2-20 nm (*Fig. 1*).

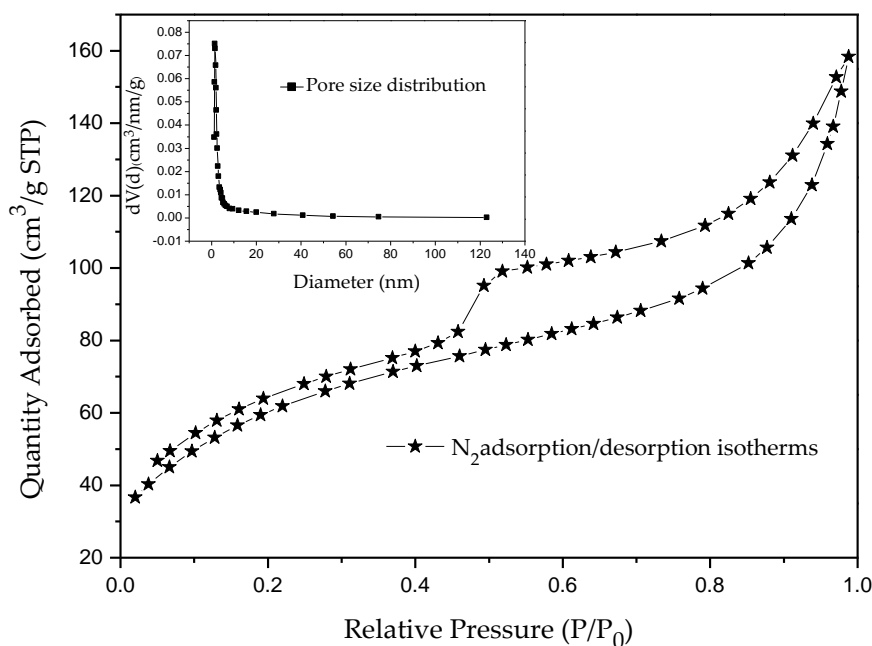


Figure 1. Nitrogen sorption isotherms of BKB—0.25 with corresponding pore size distribution

Table 1. Specific surface area parameters of BKB composite

| Composites | BET (m ² /g) | Total pore volumes (cm ³ /g) | Average pore diameter (nm) |
|------------|-------------------------|---|----------------------------|
| BKB-0.25 | 210.918 | 0.2449 | 4.645 |
| BKB-0.75 | 168.731 | 0.2032 | 4.817 |
| BKB-1.25 | 105.936 | 0.1549 | 5.850 |
| BKB-1.75 | 41.528 | 0.1066 | 10.27 |
| BKB-2.25 | 35.793 | 0.1150 | 12.86 |

As shown in *Figure 2a*, kelp biochar has a very smooth surface. And surface morphologies of BKB-0.25 (*Fig. 2b*) shows the presence of uneven structure, which suggests that Bi₂MoO₆ nanoparticles successfully grow on the surface of kelp carbon.

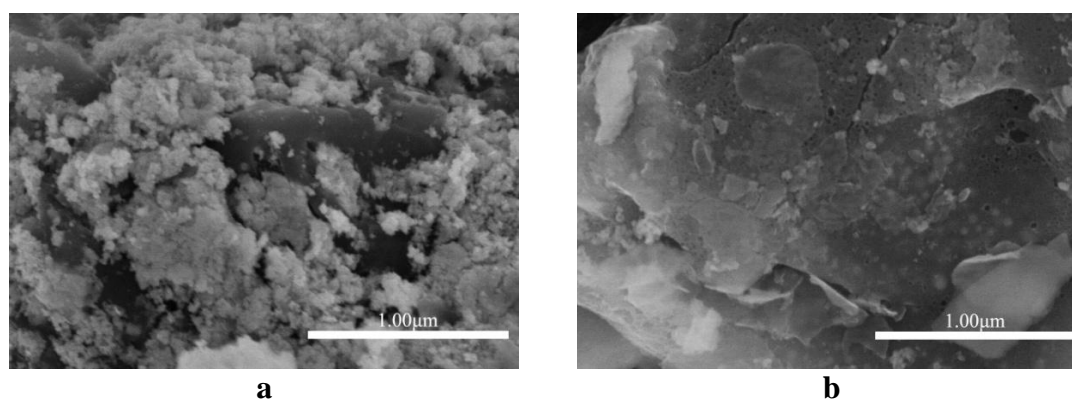


Figure 2. Surface morphologies of (a) kelp biochar, (b) BKB-0.25

Figure 3 shows the FT-IR spectrum of the kelp biochar and as-prepared Bi₂MoO₆/kelp biochar composite to investigate their chemical structures. The spectrum of pure Bi₂MoO₆ contains some strong characteristic bands such as Mo = O (~ 842 cm⁻¹) stretching vibration and the absorption at 743 cm⁻¹ is attributed to the tetrahedral stretching vibration of Mo (VI)—O groups. However, a band at 580 cm⁻¹ may be due to the bending mode of the MoO₆. Characteristic absorption bands are all observed on the as-prepared composite, indicating the presence of Bi₂MoO₆ grown on kelp biochar materials.

Information concerning the crystal structure and phase analysis of the as-fabricated materials are shown in *Figure 4*. The XRD patterns of pure Bi₂MoO₆ and BKB composite exhibit that diffraction peaks at about 2θ = 23.3°, 28.1°, 32.3°, 35.8°, 46.7°, 55.3° and 58.2° could be perfectly indexed to the (111), (131), (200), (151), (062), (331) and (191) crystal planes of orthorhombic Bi₂MoO₆ (JCPDS76-2388) respectively. This indicates that BKB composite is successfully synthesized.

A comparison of the UV–vis diffuse reflectance spectra of pure Bi₂MoO₆ and BKB composite are shown in *Figure 5*. The pure Bi₂MoO₆ exhibits a weak absorption in the visible light with range absorption edges located at 478 nm. For the BKB heterostructures, there is an enhanced absorbance in the visible-light region (λ > 400 nm) with different contents of kelp biochar added. The optical absorption edge of composite is gradually red shifted when increasing the content of kelp biochar. The

formation of the Bi_2MoO_6 /Kelp biochar heterostructures could realize a more efficient utilization of the solar energy, which is expected to become an excellent photocatalyst shortly.

A comparison of the UV–vis diffuse reflectance spectra of pure Bi_2MoO_6 and BKB composite are shown in *Figure 5*. The pure Bi_2MoO_6 exhibits a weak absorption in the visible light with range absorption edges located at 478 nm. For the BKB heterostructures, there is an enhanced absorbance in the visible-light region ($\lambda > 400$ nm) with different contents of kelp biochar added. The optical absorption edge of composite is gradually red shifted when increasing the content of kelp biochar. The formation of the Bi_2MoO_6 /Kelp biochar heterostructures could realize a more efficient utilization of the solar energy, which is expected to become an excellent photocatalyst shortly.

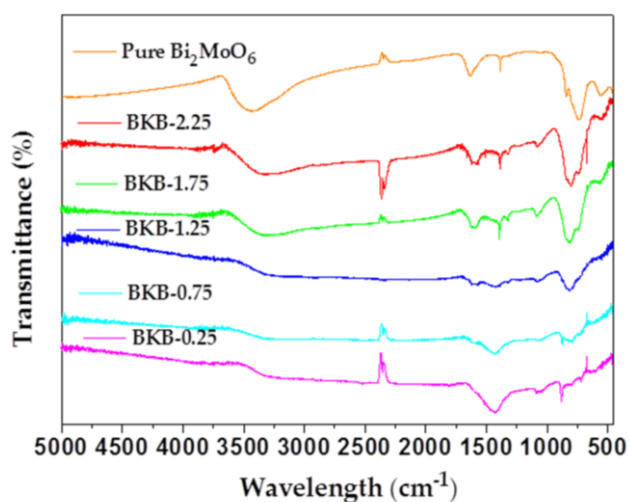


Figure 3. FTIR spectra of BKB-0.25, BKB-0.75, BKB-1.25, BKB-1.75, BKB-2.25, and pure Bi_2MoO_6

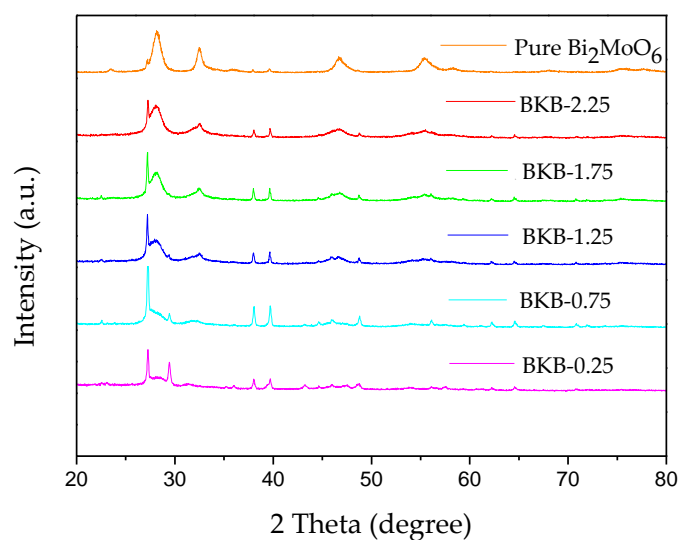


Figure 4. XRD patterns of BKB-0.25, BKB-0.75, BKB-1.25, BKB-1.75, BKB-2.25, and pure Bi_2MoO_6

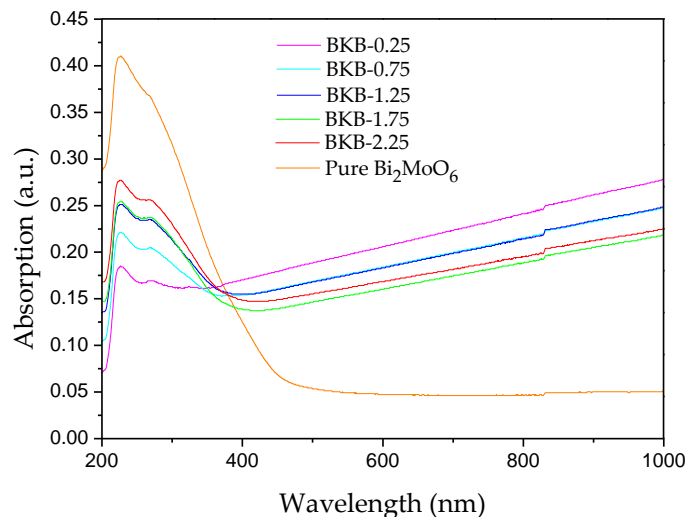


Figure 5. UV-Vis diffuse reflectance spectra of BKB-0.25, BKB-0.75, BKB-1.25, BKB-1.75, BKB-2.25, and pure Bi_2MoO_6

The removal efficiency of MB

Adsorption tests

The adsorption of methylene blue on the composite is implemented for 4 h under dark conditions without exposure to visible light illumination, and the results are represented in *Figure 6*. The increased adsorption percentage from 0.6625% to 45.28%, indicated that the adsorption will increase with the decrease of Bi_2MoO_6 content. The equilibrium adsorption capacity of MB on different Bi_2MoO_6 /Kelp biochar composite is shown in *Table 2*. It can be seen that the maximum adsorption capacity obtained by BKB-0.25 is consistent with the BET results.

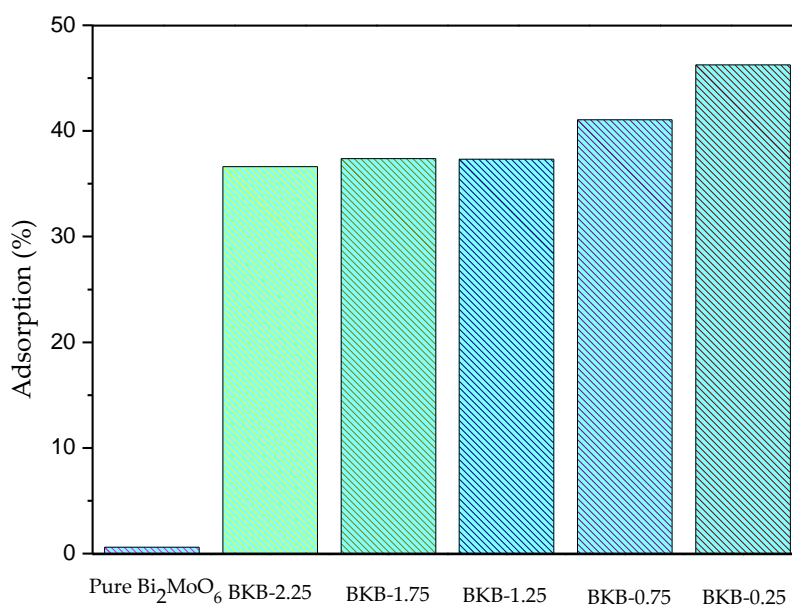


Figure 6. Adsorption of MB for BKB-0.25, BKB-0.75, BKB-1.25, BKB-1.75, BKB-2.25, and pure Bi_2MoO_6

Table 2. Equilibrium adsorption capacity of MB on samples

| Catalysts | q _e (mg/g) |
|---------------------------------------|-----------------------|
| pure Bi ₂ MoO ₆ | 2.65 |
| BKB-2.25 | 143.4 |
| BKB-1.75 | 146.4 |
| BKB-1.25 | 146.2 |
| BKB-0.75 | 160.75 |
| BKB-0.25 | 181.1 |

Photodegradation texts

On the other hand, photodegradation texts are implemented to evaluate the photocatalytic efficiency of samples under visible light irradiation. As we can see in *Figure 7*, the Bi₂MoO₆/Kelp biochar composite may have a better photocatalytic performance than pure Bi₂MoO₆. Moreover, the photocatalytic activity of the composite is remarkably enhanced with the increasing of kelp biochar content added. Significantly, BKB-0.25 composite exhibits the best catalytic activity, while the percent of MB degraded (out of total MB) is 16.11%. For comparison, blank tests are carried out at the identical conditions except for the absence of either irradiation or photocatalyst.

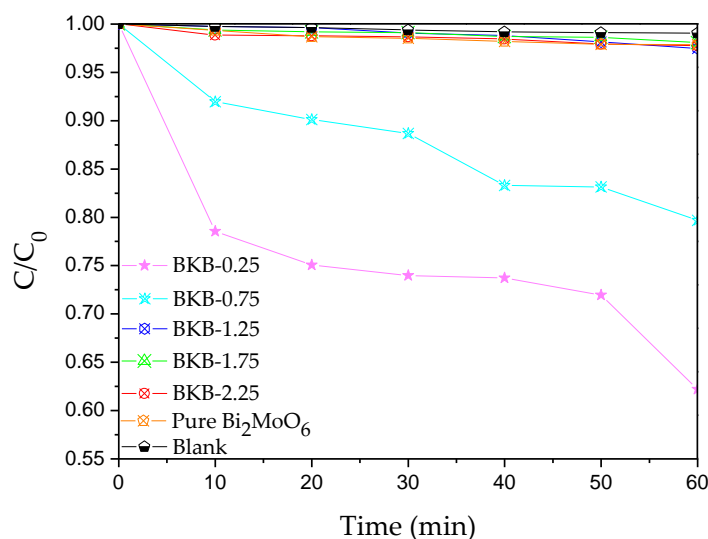


Figure 7. Degradation efficiency of MB for BKB-0.25, BKB-0.75, BKB-1.25, BKB-1.75, BKB-2.25, and pure Bi₂MoO₆

The photocatalytic degradation process of MB is studied on the basis of pseudo-first-order kinetic model, which can be expressed by *Equation 3* (Liu et al., 2017):

$$-\ln(C_t / C_0) = kt \quad (\text{Eq.3})$$

where k is apparent rate constant; C₀ is initial dye concentration in mg/L; C_t is the concentration of dye in mg/L at different time intervals.

Figure 8 shows that photocatalytic degradation processes have the good consistency with pseudo-first-order kinetic model. Moreover, pure Bi₂MoO₆ only shows a low degradation rate of 0.00045 min⁻¹. As for the BKB composite, the mass ratio of kelp biochar could greatly influence the degradation rate increasing from 0.0003 min⁻¹ to 0.0082 min⁻¹. Moreover, the maximum value is 0.0082 min⁻¹ obtained by BKB-0.25, which is up to 18.22 times higher in comparison with pure Bi₂MoO₆. As it is shown in Figure 7, the order of the MB removal efficiency is BKB-0.25 > BKB-0.75 > BKB-1.25 ≈ BKB-1.75 ≈ BKB-2.25 > pure Bi₂MoO₆. The enhanced degradation efficiency may be attributed to the synergetic effects of effective absorption as well as the heterojunction constructed between Bi₂MoO₆ and kelp biochar.

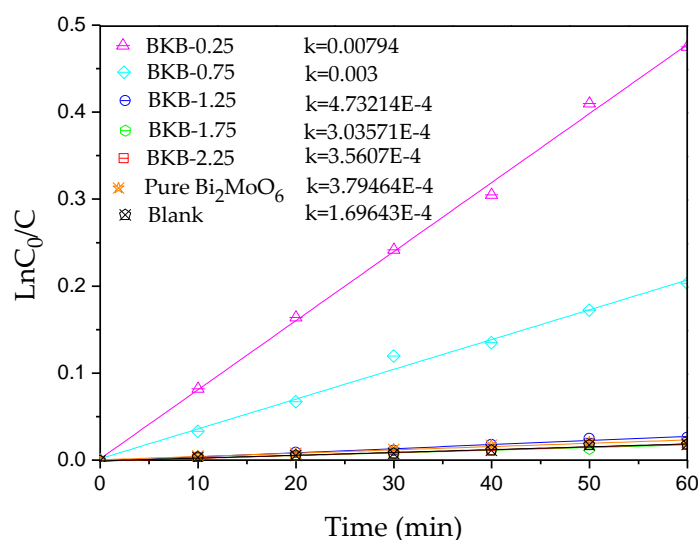


Figure 8. Kinetic process of MB degradation for BKB-0.25, BKB-0.75, BKB-1.25, BKB-1.75, BKB-2.25, and pure Bi₂MoO₆

Conclusions

In summary, a novel BKB composite has been successfully prepared via combining the pyrolysis and solvothermal method. As shown in the work, BKB nanocomposite exhibits superior removal efficiency of MB compared with pure Bi₂MoO₆, and the best degradability can be obtained by BKB-0.25 composite the best degradability. The total removal efficiency of MB on BKB-0.25 is 61.39%, which was up to 13 times higher than pure Bi₂MoO₆. Consequently, the novel composite materials with enhanced photocatalytic activity are promising candidate materials for environmental remediation.

Acknowledgements. This study was supported by the Natural Science Foundation of Zhejiang Province of China (No. LQ16D060004), Key Research and Development Projects of Zhejiang Province of China (No. 2018C02043), Demonstration Project of Marine Economic Innovation and Development of Zhoushan City of China, and Demonstration Project of Marine Economic Innovation and Development of Yantai City of China (No. YHCX-SW-L-201705).

REFERENCES

- [1] Abdelwahab, N. A., Emh, M. (2018): Synthesis and characterization of methyl pyrazolone functionalized magnetic chitosan composite for visible light photocatalytic degradation of methylene blue. – *International Journal of Biological Macromolecules* 108: 1035-1044.
- [2] Afonso, C., Cardoso, C., Ripol, A. et al. (2018): Composition and bioaccessibility of elements in green seaweeds from fish pond aquaculture. – *Food Research International*. DOI: 10.1016/j.foodres.2017.11.015.
- [3] Aravindhan, R., Madhan, B., Rao, J. R. et al. (2004): Recovery and reuse of chromium from tannery wastewaters using *Turbinaria ornata*, seaweed. – *Journal of Chemical Technology & Biotechnology* 79(11): 1251-1258.
- [4] Aravindhan, R., Rao, J. R., Nair, B. U. (2007): Kinetic and equilibrium studies on biosorption of basic blue dye by green macroalgae *Caulerpa scalpelliformis*. – *Journal of Environmental Science & Health Part A Toxic/Hazardous Substances & Environmental Engineering* 42(5): 621-631.
- [5] Cao, J., Xu, B., Luo, B. et al. (2011): Novel BiOI/BiOBr heterojunction photocatalysts with enhanced visible light photocatalytic properties. – *Catalysis Communications* 13(1): 63-68.
- [6] Chen, Y., Tian, G., Shi, Y. et al. (2015): Hierarchical MoS₂/Bi₂MoO₆ composites with synergistic effect for enhanced visible photocatalytic activity. – *Applied Catalysis B Environmental* 164: 40-47.
- [7] Chen, Y., Yu, B., Lin, J. et al. (2016): Simultaneous adsorption and biodegradation (SAB) of diesel oil using immobilized *Acinetobacter venetianus*, on porous material. – *Chemical Engineering Journal* 289: 463-470.
- [8] Choi, J., Choi, J. W., Dong, J. S. et al. (2014): Production of brown algae pyrolysis oils for liquid biofuels depending on the chemical pretreatment methods. – *Energy Conversion & Management* 86(10): 371-378.
- [9] Enniya, I., Rghioui, L., Jourani, A. (2018): Adsorption of hexavalent chromium in aqueous solution on activated carbon prepared from apple peels. – *Sustainable Chemistry & Pharmacy* 7: 9-16.
- [10] Fan, S., Tang, J., Wang, Y. et al. (2016): Biochar prepared from co-pyrolysis of municipal sewage sludge and tea waste for the adsorption of methylene blue from aqueous solutions: Kinetics, isotherm, thermodynamic and mechanism. – *Journal of Molecular Liquids* 220: 432-441.
- [11] Geng, B., Wei, B., Gao, H. et al. (2017): Ag₂O nanoparticles decorated hierarchical Bi₂MoO₆ microspheres for efficient visible light photocatalysts. – *Journal of Alloys & Compounds* 699: 783-787.
- [12] Ghosh, S. K., Bandyopadhyay, A. (2017): Adsorption of methylene blue onto citric acid treated carbonized bamboo leaves powder: Equilibrium, kinetics, thermodynamics analyses. – *Journal of Molecular Liquids* 248. DOI: 10.1016/j.molliq.2017.10.086.
- [13] Haykiri-Acma, H., Yaman, S., Kucukbayrak, S. (2013): Production of bio briquettes from carbonized brown seaweed. – *Fuel Processing Technology* 106(2): 33-40.
- [14] Jian, X., Zhuang, X., Li, B. et al. (2018) : Comparison of characterization and adsorption of biochars produced from hydrothermal carbonization and pyrolysis. – *Environmental Technology & Innovation* 10: 27-35.
- [15] Joonhyuk, C., Jaewook, C., Dongjin, S. et al. (2014): Production of brown algae pyrolysis oils for liquid biofuels depending on the chemical pretreatment methods. – *Energy Conversion & Management* 86(10): 371-378.
- [16] Lee, D. J., Cheng, Y. L., Wong, R. J. et al. (2018): Adsorption removal of natural organic matters in waters using biochar. – *Bioresource Technology* 260: 413-416.

- [17] Li, J., Liu, X., Zhuo, S., Pan, L. (2016): Novel Bi₂MoO₆/TiO₂, heterostructure microspheres for degradation of benzene series compound under visible light irradiation. – *Journal of Colloid & Interface Science* 463: 145-153.
- [18] Liu, Y., Yang, Z. H., Song, P. P. et al. (2017): Facile synthesis of Bi₂MoO₆/ZnSnO₃, heterojunction with enhanced visible light photocatalytic degradation of methylene blue. – *Applied Surface Science* 430. DOI: 10.1016/j.apsusc.2017.06.231.
- [19] Rathinam, A., Rao, J. R., Nair, B. U. (2011): Adsorption of phenol onto activated carbon from seaweed: Determination of the optimal experimental parameters using factorial design. – *Journal of the Taiwan Institute of Chemical Engineers* 42(6): 952-956.
- [20] Ross, A., Jones, J., Kubacki, M. et al. (2008): Classification of macroalgae as fuel and its thermochemical behaviour. – *Bioresour Technol* 99(14): 6494-504.
- [21] Shang, M., Wang, W., Ren J. et al. (2010): A novel BiVO₄ hierarchical nanostructure: Controllable synthesis, growth mechanism, and application in photocatalysis. – *Crystengcomm* 12(6): 1754-1758.
- [22] Son, E. B., Poo, K. M., Chang, J. S., Chae, K. J. (2018): Heavy metal removal from aqueous solutions using engineered magnetic biochars derived from waste marine macroalgal biomass. – *Science of the Total Environment* 615: 161.
- [23] Umopathy, V., Manikandan, A., Antony, S. A. et al. (2015): Structure, morphology and opto-magnetic properties of Bi₂MoO₆, nano-photocatalyst synthesized by sol-gel method. – *Transactions of Nonferrous Metals Society of China* 25(10): 3271-3278.
- [24] Velanganni, S., Pravinraj, S., Immanuel, P. et al. (2018): Nanostructure CdS/ZnO heterojunction configuration for photocatalytic degradation of Methylene blue. – *Physica B Condensed Matter* 534(April): 56-62.
- [25] Wang, S., Hu, Y., Uzoejinwa, B. B. et al. (2016): Pyrolysis mechanisms of typical seaweed polysaccharides. – *Journal of Analytical & Applied Pyrolysis* 124. DOI: 10.1016/j.jaap.2016.12.005.
- [26] Wang, S., Zhou, Y., Han, S. et al. (2018): Carboxymethyl cellulose stabilized ZnO/biochar nanocomposites: Enhanced adsorption and inhibited photocatalytic degradation of methylene blue. – *Chemosphere* 197: 20-25.
- [27] Yan, T., Sun, M., Liu, H. et al. (2015): Fabrication of hierarchical BiOI/Bi₂MoO₆, heterojunction for degradation of bisphenol A and dye under visible light irradiation. – *Journal of Alloys & Compounds* 634(1): 223-231.
- [28] Yang, K., Jiang, Y., Yang, J. et al. (2017): Correlations and adsorption mechanisms of aromatic compounds on biochars produced from various biomass at 700 °C. – *Environmental Pollution* 233: 64.
- [29] Yu, K. L., Lau, B. F., Show, P. L. et al. (2017): Recent developments in algal biochar production and characterization. – *Bioresour Technol* 246: 2-11.
- [30] Yu, Y., Wang, C., Guo, X., Paul, C. J. (2015): Modification of carbon derived from sargassum sp. by lanthanum for enhanced adsorption of fluoride. – *J Colloid Interface Sci* 441: 113-120.
- [31] Zhang, M., Shao, C., Mu, J. et al. (2011): One-dimensional Bi₂MoO₆/TiO₂ hierarchical heterostructures with enhanced photocatalytic activity. – *Crystengcomm* 14(2): 605-612.
- [32] Zhang, S., Zhang, C., Man, Y. et al. (2006): Visible-light-driven photocatalyst of Bi₂WO₆, nanoparticles prepared via complex amorphous precursor and photocatalytic properties. – *Journal of Solid State Chemistry* 179(1): 62-69.
- [33] Zhang, S. C., Yao, W. Q., Zhu, Y. F. et al. (2007): Preparation and photoelectrochemical properties of Bi₂WO₆ films with visible light response. – *Acta Physico-Chimica Sinica* 23(1): 111-115.